NeuroImage 288 (2024) 120532

Contents lists available at ScienceDirect

NeuroImage

journal homepage: www.elsevier.com/locate/ynimg

Reduced default mode network effective connectivity in healthy aging is modulated by years of education

Tibor Stöffel [a,b,*], Lídia Vaqué-Alcázar [c,d], David Bartrés-Faz [c,d], Maribel Peró-Cebollero [a,e,f], Cristina Cañete-Massé [a,f], Joan Guàrdia-Olmos [a,e,f]

[a] Department of Social Psychology and Quantitative Psychology, Faculty of Psychology, Universitat de Barcelona, Barcelona 08035, Spain
[b] Department of Nutritional Sciences, Faculty of Life Sciences, University of Vienna, Josef-Holaubek-Platz 2 (UZA II), Vienna 1090, Austria
[c] Department of Medicine, Faculty of Medicine and Health Sciences, Universitat de Barcelona, Barcelona 08036, Spain
[d] Institute of Biomedical Research August Pi i Sunyer (IDIBAPS), Barcelona 08036, Spain
[e] UB Institute of Complex Systems, Universitat de Barcelona, Barcelona 08028, Spain
[f] Institute of Neurosciences, Universitat de Barcelona, Barcelona 08035, Spain

ARTICLE INFO

Keywords:
Healthy aging
Default mode network
Dynamic causal modeling
Effective connectivity
Education
Cognitive reserve

ABSTRACT

Aging is a major risk factor for neurodegenerative diseases like dementia and Alzheimer's disease. Even in non-pathological aging, decline in cognitive functioning is observed in the majority of the elderly population, necessitating the importance of studying the processes involved in healthy aging in order to identify brain biomarkers that promote the conservation of functioning. The default mode network (DMN) has been of special interest to aging research due to its vulnerability to atrophy and functional decline over the course of aging. Prior work has focused almost exclusively on functional (i.e. undirected) connectivity, yet converging findings are scarce. Therefore, we set out to use spectral dynamic causal modeling to investigate changes in the effective (i.e. directed) connectivity within the DMN and to discover changes in information flow in a sample of cognitively normal adults spanning from 48 to 89 years (n = 63). Age was associated to reduced verbal memory performance. Modeling of effective connectivity revealed a pattern of age-related downregulation of posterior DMN regions driven by inhibitory connections from the hippocampus and middle temporal gyrus. Additionally, there was an observed decline in the hippocampus' susceptibility to network inputs with age, effectively disconnecting itself from other regions. The estimated effective connectivity parameters were robust and able to predict the age in out of sample estimates in a leave-one-out cross-validation. Attained education moderated the effects of aging, largely reversing the observed pattern of inhibitory connectivity. Thus, medial prefrontal cortex, hippocampus and posterior DMN regions formed an excitatory cycle of extrinsic connections related to the interaction of age and education. This suggests a compensatory role of years of education in effective connectivity, stressing a possible target for interventions. Our findings suggest a connection to the concept of cognitive reserve, which attributes a protective effect of educational level on cognitive decline in aging (Stern, 2009).

1. Introduction

People across the world are getting increasingly older. Societies are aging due to advances in modern medicine and lifestyle changes (Arc--Chagnaud et al., 2019). As a result, the proportion of people over 60 is estimated to have nearly doubled by 2050, however the additional years are often spent in poor health (WHO, 2022). Aging is a major risk factor for neurodegenerative diseases like Alzheimer's disease (AD) (Liu, 2022), however even in healthy (i.e. non-pathological) aging physical and mental capacity are decreasing (Arc-Chagnaud et al., 2019; Onoda et al., 2012). This demographic shift entails major challenges for societies that must accommodate their healthcare and social systems. Thus, it is important to study the processes involved in healthy aging and try to identify biomarkers that promote the conservation of functioning and increase quality of life in old age.

The human brain is affected by many structural and physiological changes in advanced age, and is key to understanding the effects of aging (Watanabe et al., 2021). Aging is associated with cortical thinning and

* Corresponding author at: Department of Nutritional Sciences, Faculty of Life Sciences, University of Vienna, Josef-Holaubek-Platz 2 (UZA II), Vienna 1090, Austria.
E-mail address: tibor.stoeffel@univie.ac.at (T. Stöffel).

https://doi.org/10.1016/j.neuroimage.2024.120532
Received 18 October 2023; Received in revised form 20 January 2024; Accepted 6 February 2024
Available online 7 February 2024

loss of white matter tracts (Vaqué-Alcázar, 2020; Watanabe, 2021; O'Sullivan, 2001; Raz and Rodrigue, 2006). Changes in cortical integrity display functional and structural correspondence, such that aging related structural deterioration has been associated with altered neural activity and cognitive functioning (Hu et al., 2014). Aging-related atrophy predominantly affects medial temporal memory regions including the hippocampus (Raz and Rodrigue, 2006; Barnes, 2009), with education and healthy lifestyle choices attenuating the effects (Nobis, 2019).

The brain's functional architecture shows robust alterations in healthy aging as well, which studies on resting-state functional connectivity demonstrate (e.g. Damoiseaux et al. 2016, Farras-Permanyer et al. 2019). Resting state functional magnetic resonance imaging (fMRI) is used to investigate the functional connectivity (i.e. functional coupling in terms of Pearson's correlations) of intrinsic spontaneous fluctuations in resting state networks (RSNs) in the absence of any experimental task manipulation. Although age-related alterations in functional connectivity have been reported for various RSNs, the most consistent findings in both healthy and pathological aging have been identified within the default mode network (DMN) (Ferreira and Busatto, 2013). The DMN is most active at wakeful rest and when simply letting the mind wander and deactivates when engaging in certain cognitive tasks (Raichle, 2015; Raichle et al., 2001). Main hubs include the inferior parietal lobules (IPL), posterior cingulate cortex (PCC), medial temporal lobes including hippocampus (HPC), and medial frontal regions. DMN activity has been associated with self-referential cognition and mental simulations based on past experiences (Buckner et al., 2008).

The network is of special interest for aging research due to its vulnerability to atrophy and patterns of hypometabolism in AD (Buckner et al., 2005) and healthy aging (Marchitelli et al., 2018). Task induced deactivation of the network is attenuated in normal aging and to a greater extent in AD, which might reflect a gradual progression of cognitive decline (Buckner et al., 2005). This is supported by findings associating reduced DMN functional connectivity in older age with lower performance in behavioral measures of cognitive function, as well as attention, and memory performance (Damoiseaux et al., 2008, 2016; Onoda et al., 2012). Whereas the effects of age and cognitive function on alterations in DMN FC appear to be modulated by educational attainment, indicating a potential protective factor (Shen et al., 2018; Chen et al., 2018; Montemurro et al., 2023).

Functional connectivity of the hippocampal DMN node seems to be particularly sensitive to aging. Andrews-Hanna et al. (2007) identified reduced functional connectivity between hippocampus and other nodes of DMN in elderly adults. These findings were complemented by Damoiseaux et al. (2016) who discovered a decrease in connectivity of posterior hippocampal formations with PCC, medial prefrontal cortex (mPFC), and lateral parietal cortex, all central hubs of the DMN.

Despite the numerous studies, the number of converging findings related to FC in healthy aging is small (Oschwald et al., 2019), with some studies finding no changes in connectivity (Koch et al., 2010) or even reporting increased connectivity with increasing age (Salami et al., 2014). Further studies suggest a non-linear relationship for FC strength and age (Farras-Permanyer et al., 2019; Montalà-Flaquer et al., 2023). The vast heterogeneity of findings may be, at least partially, attributed to the inherent absence of model-based methods in measures of FC. FC measures the spatio-temporal relationship between brain regions in the form of statistical dependence and is therefore insufficient to capture certain within network characteristics that might be key to understanding changes in healthy aging. Effective connectivity (EC) is defined as the directed influence a neural system exerts over another to generate the information flow within a network and in that way can be understood as a complementary measure to FC (Friston, 2011). EC is strictly model-based and works by comparing models of different network architectures that best explain the observed FC within a network, thereby enabling inferences about coupling between brain regions (Friston, 2011).

Dynamic causal modeling (DCM) is a framework for modeling EC (Friston et al., 2003). Compared to other methods of EC, DCM was created explicitly for the analysis of fMRI time-series data and infers causality of between region effects in a more intuitive way by using differential equations (Friston, 2011). Furthermore, DCM is considered a biologically plausible model of connectivity by taking neurovascular coupling and hemodynamics into account. Neural activity within brain regions is modeled on the neuronal level and treated as hidden states that are tuned by the strength of the connections which in turn drive a model of neurovascular coupling and hemodynamics. Taken together, these model the processes that make up the blood-oxygen-level-dependent (BOLD) signal that is measured in fMRI together with some observation noise.

With DCM, inferences on the group level can be drawn in a straightforward way by treating model parameters as random effects and analyzing second level effects with classical linear models (i.e. GLMs) (Friston et al., 2016). This allows both classification and prediction of experimental factors based on effective connectivity parameters. Though originally developed to model the stimulus-driven changes of effective connectivity in task-fMRI, Friston et al. (2014) developed spectral DCM (spDCM) to estimate effective connectivity in task-free fMRI designs. spDCM has been implemented successfully in a multitude of studies investigating resting state fMRI (e.g., Esménio et al. 2019, Lorenzini et al. 2021, Yu et al. 2021) and its validity and reliability have been ascertained (Razi et al., 2015). DCM's predictive ability together with a resting state fMRI design, which is unconfounded by performance differences across individuals, makes it a well-suited technique to identify possible biomarkers of age-related changes on a neurophysiological level.

Thus, in this study, we sought to apply resting state fMRI and to use spDCM to analyze effective connectivity in DMN in order to quantify how its functional architecture relates to healthy aging. To the best of our knowledge, this is the first study implementing spDCM to investigate the information flow within DMN in healthy aging. By understanding the information flow among DMN regions, we hope to better understand the role of each node in age-related changes in cognitive functioning. In particular, we aimed to examine the effects of healthy aging on changes in DMN effective connectivity by leveraging computational models. Additionally, we aimed to investigate the effects of attained education on aging-related variations in the DMN effective connectivity in order to identify targets of potentially protective factors.

2. Materials and methods

2.1. Participants

The data used in this study was collected as part of a prior investigation of the Department of Medicine, Faculty of Medicine and Health Sciences, University of Barcelona. The whole sample consisted of 63 subjects (40 female) in total with an age range of 48–89 years (see Table 1 for a detailed description of sample characteristics). The protocol was approved by the ethics committee of the Hospital Clínic Barcelona (October 22, 2009; Approval number: 2009-5306). All participants gave their written informed consent in accordance with the Declaration of Helsinki.

The exclusion criteria for the study included the inability to undergo neuropsychiatric testing, prior cerebrovascular accident (i.e. stroke), current diagnosis of a psychiatric disorder, cognitive deterioration, dementia or other neurodegenerative diseases, any major chronic somatic illness (such as heart failure, chronic liver disease, kidney failure, blood disease or cancer) and any conditions that would affect the eligibility to safely undergo an MRI examination. Inclusion criteria were based on the neuropsychological assessment and were defined as the absence of cognitive decline in terms of the behavioral performance in a battery of neuropsychological tests.

Table 1
Overview of sample characteristics and neuropsychological variables.

	N	*Gender (female)*	*Age*	*Years of education*	*MMSE*	*BNT*	*NART*	*WAIS (vocabulary)*	*RAVLT*
Mean	63	40	68.41	13.17	28.52	54.20	25.28	41.47	41.00
Range	–	–	48–89	8–25	24–30	43–60	16–30	17–60	17–64
SD	–	–	9.81	4.94	1.38	3.93	3.68	9.77	9.14

MMSE = Mini Mental State Exam; BNT = Boston Naming Test; NART = National Adult Reading Test; WAIS = vocabulary subscale of Wechsler Adult Intelligence Scale; RAVLT = Rey Auditory Verbal Learning Test.

A total of 12 subjects were discarded due to incomplete recordings or insufficient number of fMRI volumes (i.e. fewer than 300). The exclusion was based on simulations that have shown that the estimation accuracy of parameters in spDCM as a function of the number of time bins collected may provide accurate estimates for short runs with at least 256 or more data points (Friston et al., 2014). Furthermore, 2 subjects were removed from the analysis due to excessive head movement during the course of functional image acquisition, which exceeded the predefined maximum of 2 mm translation or 2° rotation.

2.2. Neuropsychological scales

The neuropsychological examination was designed with the goal of assessing a comprehensive measure of healthy cognitive levels in a variety of cognitive domains. The assessment involved the following instruments: Mini-Mental-State-Examination (MMSE) (Folstein et al. 1975; Tombaugh and McIntyre, 1992); National Adult Reading Test (NART) (Nelson, 1982; Nelson and Willison, 1991); the vocabulary subscale of the Wechsler Adult Intelligence Scale (WAIS) (Lezak et al., 2004); Boston Naming Test (BNT) (Kaplan et al., 1983, 2001); and Rey Auditory Verbal Learning Test (RAVLT) (Rey, 1964). These scales made up the inclusion criteria, i.e. a neuropsychological evaluation to verify normal cognitive functioning in relation to age standardized norms. Hence, only subjects with scores considered clinically insignificant were included in this study.

2.3. MRI acquisition

MRI data were collected using a Siemens Magnetom TrioTim Syngo 3 Tesla scanner (Erlangen, Germany) at the Unitat d'Imatge per Ressonància Magnètica IDIBAPS of Hospital Clínic in Barcelona (Spain). A high-resolution 3D T1-weighted structural image was obtained using a MPRAGE protocol (repetition time (TR) = 2300 ms, echo time (TE) = 2.98 s, 240 slices, pixel size = 1 × 1 mm, slice thickness = 1 mm, flip angle = 9°, field of view (FOV) = 256 mm). Functional images were acquired as 10-minute (300 volumes) whole-brain resting state fMRI scans using a T2*-weighted echo-planar imaging (EPI) BOLD sequence (TR = 2000 ms, TE = 16 ms, 40 slices, pixel size = 1.7 × 1.7 mm, slice thickness = 3 mm, interslice gap = 25 %, flip angle = 90°, FOV = 220 mm). Participants were instructed to lie down with their eyes closed and not fall asleep.

2.4. Functional connectivity pre-processing and analysis

To investigate the temporal and spatial characteristics of low frequency fluctuations in terms of resting-state functional connectivity, spatial independent component analysis (ICA) was employed using tools provided as part of the FMRIB Software Library (FSL v6.0.5.2; https://fsl.fmrib.ox.ac.uk/fsl/) (Beckmann et al., 2005). Pre-processing steps included: removal of first five volumes (10 s) to allow steady state magnetization to develop as well as for subjects to adjust to the loud scanner noise; slice-timing correction to account for differences in slice acquisition times; McFlirt motion correction using rigid-body transformations of each volume to the middle volume as a reference; Co-registration to each high-resolution structural image and subsequent non-linear normalization to MNI standard space in a two-step procedure; spatial smoothing with a 5 mm full width at half-maximum (FWHM) smoothing kernel; band-pass filtering (0.01–0.08 Hz) to retain only low-frequency BOLD fluctuations which reflect spontaneous neural activations in resting state (Biswal et al., 1995; Soares et al., 2016); 80 % probability tissue maps generated from segmenting white matter (WM), grey matter, and cerebrospinal fluid (CSF), were used to extract the mean time-series of WM and CSF; and finally, nuisance regression of all six motion parameters together with mean CSF and WM time-courses was performed.

FSL's MELODIC algorithm was used to infer on resting-state connectivity patterns across subjects and acquire a group specific map of DMN regions using a temporal concatenation ICA approach (Beckmann et al., 2005). This is a multivariate data-driven approach that decomposes the fMRI signal into its different sources of variability (i.e. components) while maximizing the independence between them. The results are spatial maps of functionally connected brain regions. We used MELODIC's automatic Bayesian dimensionality estimation technique in order to uniquely decompose the data so that each component very likely corresponds to exactly one physiological or physical source (Beckmann and Smith, 2004). Using this approach, we extracted 112 independent components. Dual regression was used to generate subject specific sets of spatial maps corresponding to each independent component in a two-step procedure (Nickerson et al., 2017). First the spatial components were regressed onto each subject's 4D dataset to extract time-courses corresponding to each spatial independent component. Afterwards, the time-courses were regressed onto each 4D dataset resulting in subject-specific spatial component maps. We then used a term-based meta-analysis map summarizing results from 777 studies (Neurosynth; Yarkoni et al. 2011) (threshold: P(FDR) < 0.01) using the term 'default mode' to robustly identify the IC map corresponding to the DMN.

Inference on the group level was performed by taking the subject-specific maps to a second-level analysis using SPM12 (Version 12.5; https://www.fil.ion.ucl.ac.uk/spm/). A one-sample t-test was computed to assess regions of the DMN that were consistent across participants. Additionally, age, gender, level of education, and the interaction of age and education were added to the analysis as covariates. Results were considered significant at a p-value < 0.05 family-wise error corrected (FWEc) using SPM's whole brain cluster-wise threshold based on random field theory.

2.5. Effective connectivity pre-processing and analysis

For the estimation of DMN effective connectivity, we performed a second pre-processing and analysis pipeline using SPM12. The following pre-processing steps were carried out: removal of the first five volumes (10 s); slice-timing correction to the middle-acquired slice; motion estimation and correction by realigning all slices to the mean image; unwarping to remove movement induced variance caused by the susceptibility-by-movement interaction; co-registration to high-resolution T1-weighted images and subsequent normalization to a MNI standard space template; smoothing using a 5 mm FWHM gaussian kernel; nuisance regression of all six motion parameters as well as CSF and WM time-courses. After preprocessing all images were visually inspected to ensure correct normalization.

Resting state effective connectivity within DMN was estimated using

spectral Dynamic Causal Modeling implemented in SPM12 (DCM Version 12.5) (Friston et al., 2014). spDCM estimates the cross-spectral densities of the BOLD signals, which is the cross-correlation in the frequency domain. This provides a simple and efficient way of estimating models of effective connectivity in resting-state fMRI.

First, we defined brain regions of interest (ROIs) based on the sample specific DMN map retrieved with ICA (see above). Cluster peaks within a meta-analytic mask generated with Neurosynth and corresponding to the 'default mode' (see above) were used to localize centers for each ROI. We pursued this approach in order to estimate the relative specificity of the functional brain activity identified with ICA and the DMN (see e.g., Wang et al. 2020). Seven regions resembling key nodes of the DMN were identified (Raichle, 2015), namely the right inferior parietal lobule (rIPL), the left inferior parietal lobule (lIPL), the PCC, the right middle temporal gyrus (rMTG), the left middle temporal gyrus (lMTG), the left hippocampus (HPC), and the medial prefrontal cortex (mPFC). The ROIs were masked by an 8 mm sphere and the first principal component from each ROI was extracted as a summary time-series.

In the next step we defined the connectivity matrix of the forward model. We adopted an exploratory approach and started with a fully connected model which included all biologically plausible connections for each subject, i.e. all 49 connections between ROIs and 7 recurrent self-connections. In a subsequent step, the models of each subject were inverted, and the posterior estimates of the parameters (i.e. connection strengths) were iteratively updated so that the generated time series best explained the observed data. Using a technique called Variational Laplace, parameters with the best trade-off between model fit and complexity were determined (Friston et al., 2007). Explained variance of estimated first-level DCMs was inspected to ensure convergence (*Mean* = 87.97 %; *SD* = 3.61 %; *Range* = 74.66–95.11 %). No model was excluded due to poor data fit. Moreover, all models displayed non-trivial neural parameters with 90 % credible intervals (i.e. Bayesian confidence intervals) that excluded zero.

After inverting each subject's DCM, we investigated group-level commonalities in connectivity parameters and effects associated with healthy aging using the Parametric Empirical Bayes (PEB) approach, which is a Bayesian Framework for group level statistics of DCMs (Friston et al., 2016). PEB takes the connectivity parameters from the first level DCMs to the group level and models them as a linear combination (GLM) of a group mean, between-subject differences modeled by covariates of interest, covariates of no interest, and random effects variability (Zeidman et al., 2019b). We set up a design matrix with age and the interaction of age and education as our effects of interest and included gender and level of education as covariates of no interest. All covariates were mean centered. Having estimated the group level parameters, we applied Bayesian Model Reduction in an exploratory fashion comparing all nested models (i.e. models with certain connections switched 'off') and iteratively discarding parameters that did not contribute to model evidence. This is essentially a greedy-search algorithm. Afterwards, a Bayesian Model Average (BMA) was computed over the remaining 256 models, providing posterior parameters estimates and their covariances. In line with prior research, credible intervals were computed and parameters with 90 % credible intervals not including zero were deemed large enough to be of interest (Almgren et al., 2018; Lorenzini et al., 2021). However, due to the large number of connections we focused on EC parameters with an associated posterior probability > 0.99.

To further investigate the effective connectivity parameters associated with healthy aging, we conducted a leave-one-out cross validation. We assessed the predictive validity of our parameter estimates, i.e. whether the effect sizes were large enough to be able to predict the subjects' age from their neural response. PEB models were fitted to all but one subject and the age for the left-out subject was predicted. This was repeated over each subject and the accuracy of the prediction of out of sample estimates was recorded. A correlation between actual and predicted age was calculated and tested for significance. A correlation coefficient with an associated p-value < 0.05 was deemed significant.

We went on to study the relationship between effective connectivity estimates related to healthy aging and variability in the neuropsychological assessment. To understand the relative influence of different neuropsychological subscales or aspects of cognitive functioning on each subject's changes in network connectivity, we performed canonical variate analysis (CVA) (Darlington et al., 1973). Canonical vectors with an associated p-value < 0.05 were considered significant.

3. Results

3.1. Neuropsychological variables

Even though the neuropsychological variables in our sample where within the sub-clinical range, we were interested whether the performance was declining with age. Therefore, we performed a multiple regression analysis between the neuropsychological performance and age ($F(7,37) = 2.775$; $R^2 = 0.3442$; $p = 0.02$). Out of all neuropsychological scales only RAVLT scores were associated with age (β = -0.5863; t = -2.875; $p = 0.0067$), while accounting for gender and level of education (see Fig 1). An additional regression model examining the association of age, gender, and level of education with RAVLT, revealed that RAVLT scores were furthermore positively associated with level of education ($\beta = 2.9034$; $t = 2.32$; $p = 0.025$; $F(4,44) = 7.664$; $R^2 = 0.411$; p = <0.001), while the negative association with age remained (β = -0.4556; t = -2.72; $p = 0.0093$). Gender ($\beta = 3.1456$; $t = 2.145$; $p = 0.15$) as well as the interaction of age and education was not significantly associated to RAVLT test scores ($\beta = 0.0025$; $t = 0.021$; $p = 0.983$).

3.2. Functional connectivity

The main goal of the ICA was to retrieve a sample specific map of the DMN. A one-sample t-test of the first level DMN spatial IC maps revealed several significant clusters at the group level (P(FWEc) < 0.05). The main regions consisted of the bilateral angular gyri within the inferior parietal lobules, PCC, bilateral middle temporal gyri, medial prefrontal cortex, and left hippocampus (see Table 2 & Fig. 2).

3.3. Effective Connectivity

In order to understand the importance of DCM results an essential distinction between directed extrinsic connections between regions and intrinsic self-connections must be made. Whereas the former represents what we know as effective connectivity, i.e. the effect one region exerts over another in units of Hz (rates of change), self-connections reflect the susceptibility of a node in a network to incoming directed connections from other regions (i.e. extrinsic afferents) (Zeidman et al., 2019a). This change in susceptibility is parameterized as unitless log-scaling parameters that modulate the default self-inhibition of a region set at -0.5 Hz.

In terms of coupling, the PEB analysis showed that aging was related to an overall strong coupling between regions of the posterior DMN, including left and right IPL and PCC, with HPC and rMTG (see Fig. S1). rMTG showed the most extensive coupling within the network with connections to four of the six remaining nodes susceptible to aging.

Excitatory effective connections (i.e., when a region's activity causes an increase in activation in their efferent destination) associated to aging were discovered from PCC to rIPL (52), lIPL to rMTG (75), rMTG to lMTG (83), and lMTG to PCC (85) (see Fig. 3a). Inhibitory effective connections, which are defined to cause a decrease in activity in the receiving region depending on activation of the source region (or in other words to have a reduced influence over another region), were detected at a higher number. Inhibitory connections associated to aging included from PCC to rMTG (54), PCC to HPC (56), mPFC to lMTG (62), rMTG to PCC (78), rMTG to rIPL (80), rMTG to lIPL (80), and HPC to lIPL (95). Apart from effective connectivity parameters, there was also a self-connection parameter observed with a very high posterior probability

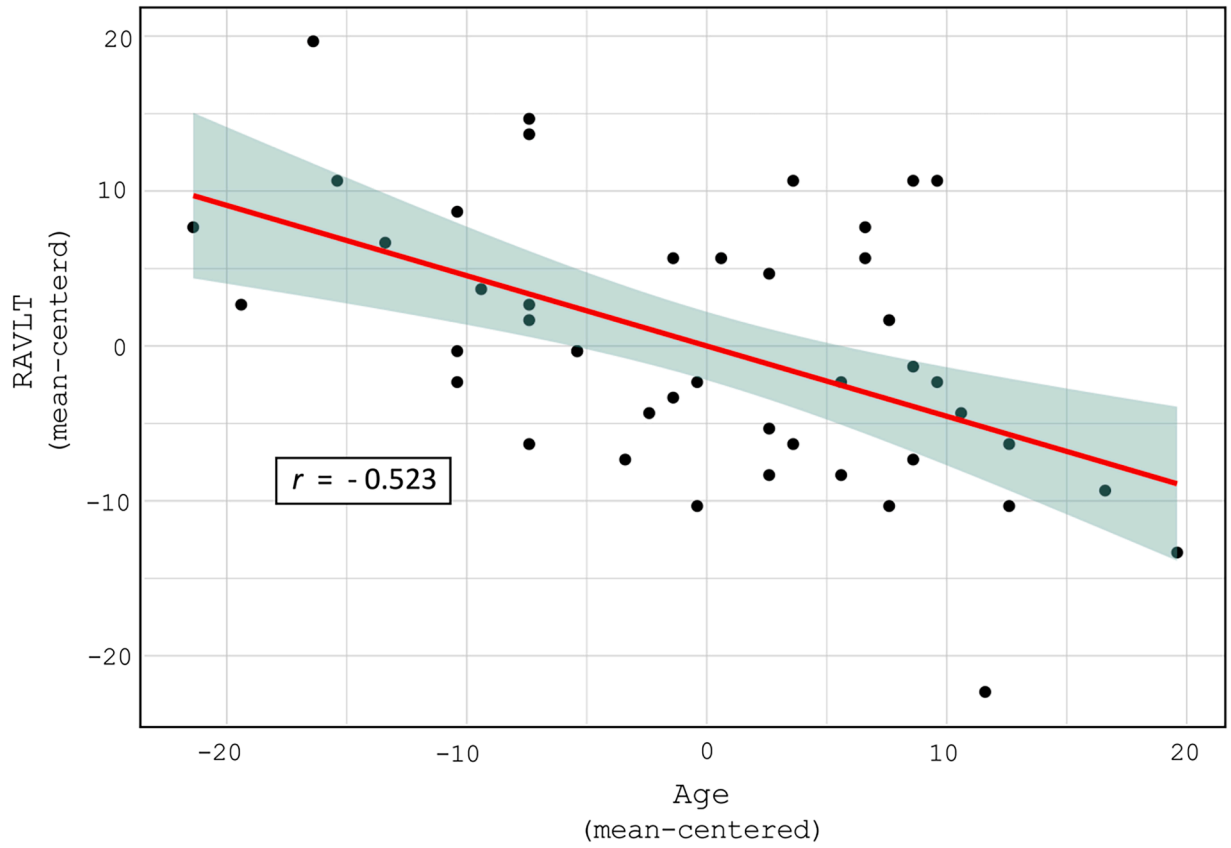

Fig. 1. Results from a multiple regression analysis of age with each scale of the neuropsychological assessment, gender and level of education as predictors. RAVLT scores sig. predicted age ($p = 0.0067$). Regression line is shown in red. Shaded area shows 95 % confidence area of the regression line. Pearson's $r = -0.523$. RAVLT = Rey Auditory Verbal Learning Test.

Table 2
ICA group map peak regions within a term-based meta-analytic mask (term: 'default mode') resembling key nodes of the DMN. x, y, z = MNI coordinates.

Peak Region	*x*	*y*	*z*	*T*
PCC	-6	-48	38	15.8
Left Inferior Parietal Lobule	-52	-58	38	11.73
Right Inferior Parietal Lobule	46	-58	36	9.84
Right Middle Temporal Gyrus	62	-6	-26	6.66
Left Hippocampus	-24	-36	-16	5.98
Medial Prefrontal Cortex	18	58	18	5.95
Left Middle Temporal Gyrus	-61	-22	-16	5.31

for the HPC (98). With increased age the sensitivity of the hippocampus towards inputs from other nodes of the DMN was increasingly reduced, disconnecting it from the network's influence.

In order to assess the meaningfulness of the neural parameters linked to healthy aging, we carried out a leave-one-out cross validation for the parameters with an associated posterior probability > 0.99 and it was examined whether the neural parameters were able to predict out of sample values of age. The predicted values for age were significantly correlated with the samples' actual age values ($r(47) = 0.30$; $t(47) = 2.13$, $p = 0.039$) meaning that the spDCM parameters were predictive of age-related changes in neural network activity (see Fig. 4). spDCM parameters associated with the interaction of age and level of education attained over the course of life revealed more long-range coupling for DMN nodes with more remote regions (see Fig. S2). The pattern of information flow within DMN implies more engagement of frontal regions, rMTG to be a less prominent network hub, shifting towards PCC as a key modulatory node of network activity with many inhibitory extrinsic connections (see Fig. 3b).

Excitatory connectivity parameters comprised connections from mPFC to HPC (210), lIPL to mPFC (219), lMTG to rMTG (236), HPC to PCC (239), and HPC to LIPL (242). Inhibitory connections were discovered for the connections from PCC to mPFC (198), rIPL (199), lMTG (202), and HPC (203). Further inhibitory connections were found from rMTG to lIPL (228) and from HPC to rMTG (243). The self-connection parameter of the lIPL (221) was associated with the interaction term, suggesting increased susceptibility to network inputs.

Canonical variate analysis of the multivariate relationship between DCM effective connectivity estimates associated with healthy aging and neuropsychological performance in different cognitive domains showed no significant canonical correlations for any canonical vectors.

4. Discussion

Societies are aging increasingly and with this comes an increased risk for diseases such as dementia. However, also in non-pathological aging cognitive functioning can be deteriorating for a large portion of the elderly community. Finding biomarkers that code for age-related changes in brain physiology could help to better understand the detrimental effects on cognitive functioning with higher age. Importantly, localization of central hubs that drive these changes would ease the identification of potential targets for interventions. The aim of this paper was to identify changes in information flow at rest within the default mode network that were driven by increasing age in a sample ranging from 48 to 89 years. By investigating the information flow and coupling architecture, we sought to identify the relative contribution and involvement of each node.

The results from our spDCM with age as a continuous predictor show that every DMN node is affected by changes in effective connectivity, however some more prominently than others. For the right MTG

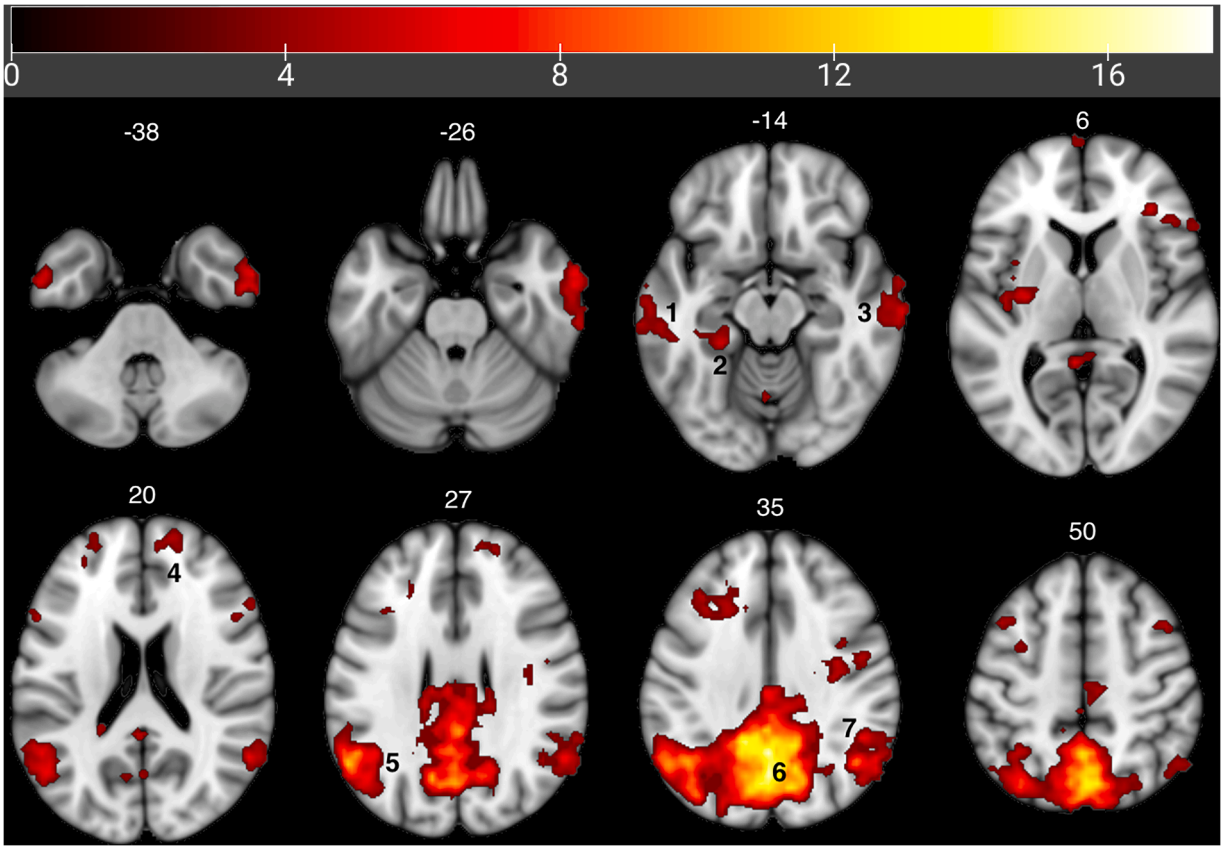

Fig. 2. Axial slices of spatial independent component resembling the DMN. Images have been thresholded at P(FWEc) < 0.05. Color bar displays t-values. Slices are displayed in neurological convention. Numbers in white denote slice z-coordinate. Numbers in black denote ROIs: (1) lMTG = left middle temporal gyrus; (2) HPC = hippocampus; (3) rMTG = right middle temporal gyrus; (4) mPFC = medial prefrontal cortex; (5) lIPL = left inferior parietal lobule; (6) PCC= posterior cingulate cortex; (7) rIPL = right inferior parietal lobule.

together with the left HPC, we found efferent connections inhibiting activity in the left and right IPL as well as the PCC. All three regions are part of the posterior DMN. These regions are the first to show AD related decline in FC within the DMN (Damoiseaux et al., 2012). A similar pattern has been identified in healthy aging, albeit at a slower rate (Jones et al., 2011). Jones et al. (2011) further discovered that changes within posterior DMN FC were associated to cognitive performance in healthy aging as well as in AD, suggesting these regions to be essential in tracing impending cognitive dysfunction. The breakdown in communication between the IPL and the PCC has been linked to disrupted metabolism (i.e. hypometabolism) in dementia-related pathologies, such as mild cognitive impairment and AD (Marchitelli et al., 2018). In healthy aging, reduced metabolism was mainly detected for the PCC, and moreover, this hypometabolism was predictive of cognitive decline (Mosconi et al., 2007). This suggests the MTG and HPC to be driving factors in the downregulation of posterior DMN nodes that could explain the widely observed decrease in functional connectivity in the literature.

The PCC builds a core memory network with temporal regions including the MTG and HPC (Svoboda et al., 2006). Rabin et al. (2010) discovered that the MTG together with the PCC and the HPC were associated with autobiographical memory or “thinking about past experiences” in general. The same regions have been implicated in encoding long term memories (Wimber et al., 2010). Milton et al. (2012) associated the MTG and PCC with autobiographical memories as well and found changes in effective connectivity of the right hemispheric MTG for patients suffering from a form of epileptic amnesia that impairs memory recall.

Interestingly, using ICA in a task-based design to probe biographical memory retrieval, Ge et al. (2014) found the middle temporal gyri to be increasingly recruited for older compared to younger participants when recalling positive memories. The authors concluded that this might signify an overcompensation, in the way that older individuals would need to recruit further resources to attain a similar result. This is in line with Damoiseaux et al. (2012) who discovered in a longitudinal study of AD patients that the ventral DMN subnetwork, which mainly includes the temporal lobes, initially showed increased FC that deteriorated in the later stages of the disease.

Notably, in our study only the right MTG appeared to reduce its influence over the posterior DMN, with a reciprocal inhibitory coupling to the PCC. Age-related decrease in FC between ventral and posterior DMN regions has already been discussed and these inhibitory connections would explain the observed changes in FC. What remains to be elucidated is the lateralization in EC for temporal lobe regions, more specifically the MTG. Although there have been some studies associating age- and memory-impaired disorders with a functional lateralization in DMN nodes (e.g. Banks et al. 2018, Milton et al. 2012, Svoboda et al. 2006), these findings have been inconsistent with regards to a certain hemispheric dominance and should profit from further investigations focusing on lateralization of functional and effective connectivity changes. One has to keep in mind that lateralization found in the FC of brain networks must not necessarily coincide with the underlying EC structure that drives the observed network connectivity.

The hippocampus is critical to memory function, which is considerably impaired in the elderly population probably due to dysfunctional synaptic plasticity in medial temporal lobe regions (Torres and Cardenas, 2020). One of the key findings in the present study is that with increasing age the HPC appears to functionally segregate itself from the DMN. This is reflected by the increasingly inhibitory self-connection parameter. When using Regional Homogeneity (ReHo), a measure of local connectivity of neighboring voxels, Harrison et al. (2019)

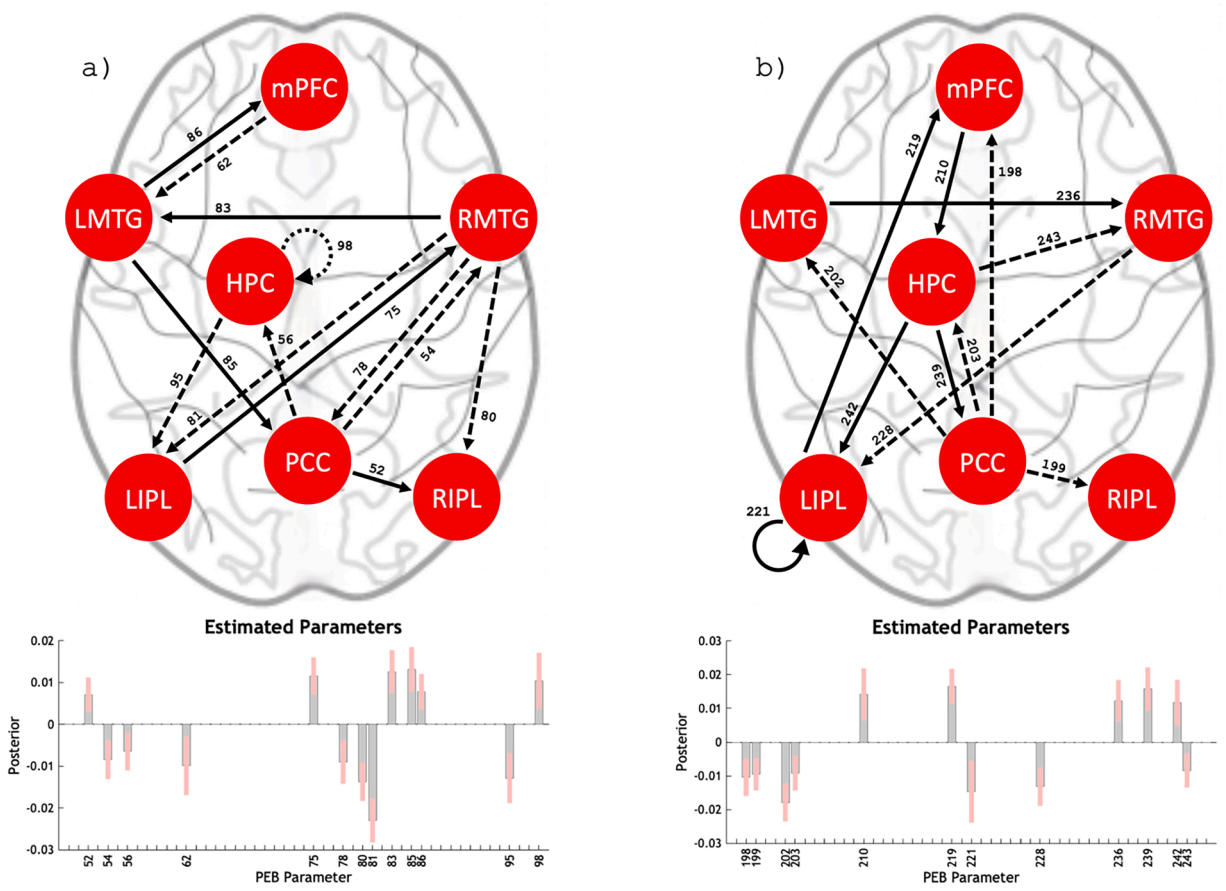

Fig. 3. Group effective connectivity wiring diagrams (upper half). Straight arrows denote directed connections, curved arrows self-connections. Solid lines represent excitatory connections, dashed lines inhibitory connections. PEB effective connectivity parameters with posterior probability > 0.99 that the parameters are not 0 (lower half). PEB parameter numbers (values on the x-axis) correspond to the connectivity parameters in the wiring diagrams. (A) spDCM parameters associated with healthy aging. (B) spDCM parameters associated with the interaction of age and level of education. Red error bars represent 90 % credible intervals. Units of PEB parameters are in Hz for directed connections. Parameters for self-connections are unitless log-scaling parameters scaling the default value of -0.5 Hz. PEB = parametric empirical bayes; spDCM = spectral dynamic causal model.

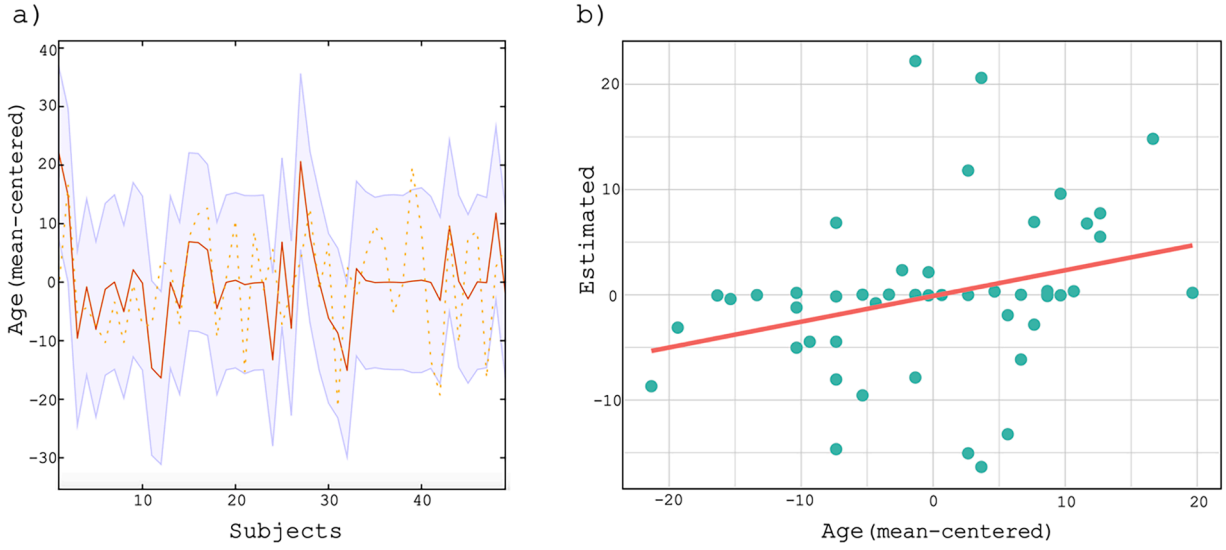

Fig. 4. Leave-one-out cross validation on the group-level PEB parameters associated with healthy aging. A) Actual age plotted as an orange dotted line for each subject with corresponding estimate (solid orange line) and 90 % confidence interval (shaded area) based on connectivity parameters. B) Subjects' actual age plotted against cross validation estimates ($r(47) = 0.30$; $t(47) = 2.13$, $p = 0.039$) with a line of best fit. PEB = parametric empirical bayes.

discovered that in elderly adults HPC ReHo was increased whereas HPC FC was decreased. Both measures of connectivity were related to AD pathology and higher ReHo within HPC was predictive of worse memory performance in neuropsychological tests. Taken together, they interpreted their findings as an age-related functional isolation in terms of long-range disconnection that lead to increased local connectivity of HPC and decreased memory performance. Montalà-Flaquer et al. (2023) also found increased ReHo in hippocampal regions in healthy aging, however they interpreted their findings as a possible compensatory mechanism that is supposed to offset functional impairment, as they found no relationship to cognitive performance measured with a battery of neuropsychological tests. The increased functional segregation of HPC observed in the current study demonstrated by both age-related disconnection from the network as well as inhibitory connections to PCC and LIPL could explain how the functional isolation emerges. Moreover, this pattern might be an early precursor of mild cognitive impairment (MCI) pathology, which is associated with reduced activity in left HPC together with reduced PCC, left IPL, and left MTG activity (Vogelaere et al., 2012).

To summarize, the observed pattern of EC in this study is well in line with findings from studies investigating both functional and structural changes with advancing age. These studies, together with our findings, convey a picture of disrupted DMN information flow for regions essential in memory functioning. Andrews-Hanna et al. (2007) discussed a two-factor model of aging-related deficits that comprises memory disruption linked to AD which is hypothesized to be grounded in medial temporal lobe deficits and secondly, executive dysfunction linked to frontal-striatal dysfunction. Our findings fit well within the former part of this theoretical model. At this point it should be stressed that among the different neuropsychological scales only RAVLT scores were associated to age (i.e. verbal memory decreased with age), further substantiating the decay of memory function even in non-pathological aging.

We tested the predictive validity of our model parameters, i.e. we assessed whether we could predict subjects' age based on their information flow between DMN nodes. We were able to conclude that the effect size estimated by spDCM was sufficiently large to predict out-of-sample subjects' age above chance. However, with a Pearson's $r = 0.3$, there's still a lot of variability left to be explained. Nonetheless, the model serves as a potential predictive biomarker of brain changes in healthy aging.

For our second research question, we examined possible moderating effects of years of education. We detected changes in both couplings and signs of EC parameters. Most notably, we found that the excitatory EC parameters associated with the moderation are almost exclusively concentrated around the HPC. Compared to the effective connectivity architecture of parameters related to healthy aging, the interaction with educational attainment appears to reverse or counteract the inhibiting role of HPC and RMTG on the bilateral IPL and the PCC. The HPC inhibits the right MTG, which in turn is also expressing fewer inhibiting EC parameters to posterior DMN nodes. Additionally, the HPC displays two outgoing excitatory connections to the PCC and left IPL. Together with the mPFC, that forms an excitatory efferent to the HPC, these regions build an excitatory cycle. Furthermore, the mPFC appears to take a moderating role in the network with both excitatory and inhibitory afferents from posterior DMN nodes and an outgoing excitatory connection to the HPC.

When comparing MCI patients with memory problems to education matched healthy elderly, Vogelaere et al. (2012) found a left lateralized increase in HPC, IPL, and PCC activity for healthy elderly, proposing a possible compensatory role of these regions. Especially the PCC has been shown to play a key role in supporting cognitive function and is predictive of cognitive performance (Lin et al., 2016). Sala-Llonch et al. (2015) further highlighted the importance of the prefrontal cortex as a core region related to compensatory mechanisms to age-related functional decline. For instance, decline in FC between mPFC and HPC was predictive of poorer global performance in older adults and this was linked to a gene variation which is associated to worse cognitive decline and cognitive impairment in Alzheimer's disease (Franzmeier et al. 2021). Activity within the left posterior parietal lobe, the PCC, and the mPFC has been predictive of working memory performance in a study investigating age-related alterations in DMN (Sambataro et al., 2010). This finding is further corroborated by Andrews-Hanna et al. (2007) who found that the FC between PCC and mPFC was associated with higher cognitive performance in older adults. In line with that, a study using MEG found that high performing elderly showed increased activation within left PFC regions, a possible sign of compensation of brain function (Lin et al., 2018). This indicates that in healthy elderly with additional years of education, the DMN effective connectivity is associated with excitatory coupling to regions that are essential for cognitive performance and memory functioning.

Our findings can be interpreted in the context of cognitive reserve. Cognitive reserve was defined to account for the high heterogeneity regarding susceptibility to age and dementia-related brain changes on cognitive functioning (Stern, 2009; Stern et al., 2020). Essentially acting as a buffer from decline. Importantly, most of the processes that are thought to underlie cognitive reserve can be modified across the lifetime (e.g. proxies such as education, physical exercise, social engagement). This highlights how important it is to continue to work on these aspects across the lifespan and presents opportunities for early interventions. Reserve is at its core a moderation of aging or pathology-related biomarkers and sociobehavioral proxies, such as aging and educational attainment across the lifespan.

This study and its design entailed some limitations. We set out to investigate changes in aging, covering the age-range between 48 and 89 years. Prior work suggests that aging related effects do not only apply to the transition from general adulthood to older age, instead it is more likely for different cognitive aspects to follow an inverse U-shape with peaks between 20 and 45 years (Hartshorne and Germine, 2015). We applied strictly linear modeling to our EC parameters on the group level and therefore might be missing effects that follow a higher order (i.e. non-linear) relationship with aging (see Farras-Permanyer et al. 2019, Montalà-Flaquer et al. 2023). This should be considered by future research. Furthermore, our study design was cross-sectional and any changes we found in relation to aging could potentially be confounded by sample specific differences between participants. Future work should employ longitudinal designs to investigate whether these aging related changes in DMN EC can be replicated. In addition, including follow up examinations could have helped determine whether the participants remained healthy over a significant period of time. This would allow additional insight into which factors could be attributed to aberrations seen in healthy aging and which might be symptoms of pre-clinical age-related neuropsychological deteriorations as seen under AD. Besides, this study focused strictly on the DMN as a network of interest for healthy aging. Therefore any findings and conclusions discussed here are limited to this network. It would be interesting however, to see whether these effects generalize to other resting-state brain networks.

A caveat to our findings is that the parameter effect sizes were rather small in the range of 0.01–0.02 Hz. We chose a correlational design which is known to produce smaller effect sizes in contrast to designs that compare means. However, we intentionally chose a regression model in order to capture the whole range of age in our sample. Additionally, our parameters were associated with a very high posterior probability ($>$ 0.99) and our effect sizes were sufficiently large to predict out-of-sample covariates in a leave-one-out cross-validation.

Finally, our EC parameters did not show a multivariate relationship to any of our neuropsychological variables. However, we identified a negative relationship of age and a positive relationship of level of education with performance on the memory test RAVLT. Identifying age-related brain changes that covary with levels in cognitive performance could provide a deeper mechanistic understanding. By deliberately excluding any participants that were in the clinical spectrum of a

neuropsychological examination, we were left with very little variation in these tests between participants. A different design that incorporates scores within the clinical range might be more suitable to detect associations between changes on the brain and behavioral level. It will also be important for future work to incorporate task-fMRI to investigate the relationship of age-related network changes and memory. Using a larger sample and combining rs-fMRI with a memory task could confirm our initial findings and provide us with a more comprehensive understanding of the individual involvement of DMN nodes susceptible to age-related changes and memory.

5. Conclusion

In conclusion, we identified how the information flow within the DMN changes in association to healthy aging. We found distinct changes within temporal lobe and posterior DMN regions that are in line with age-related memory impairment and functional disconnection observed in prior studies. Moreover, we identified changes in EC parameters susceptible to the moderation of healthy aging and years of education. We found that education reversed many of the inhibitory connections associated with aging, especially concerning the mPFC, HPC, and LIPL. These regions formed a cycle of excitatory connections, possibly displaying the effects of cognitive reserve on the brain level. To the best of our knowledge we were the first (i) to identify coupling architectures and patterns of information flow within the DMN in relation to healthy aging, and (ii) to identify how years of education (as a proxy for cognitive reserve) moderates these connections. Future work should seek out to further investigate resting state network changes in healthy and pathological aging by incorporating different networks and try to validate these changes on a behavioral level.

Funding

This study was supported by the Erasmus+ grant for Traineeship Mobility in higher education (academic year: 2021/22; sending institution: University of Vienna) as well as the Group of Quantitative Psychology, members of the Generalitat de Catalunya's SGR 366 Consolidated Research Group (GRC), and it was made possible by the PSI2013-41400-P project of the Spanish Government's Ministerio de Economía y Competitividad.

CRediT authorship contribution statement

Tibor Stöffel: Conceptualization, Methodology, Software, Formal analysis, Writing – original draft, Writing – review & editing, Visualization. **Lídia Vaqué-Alcázar:** Investigation, Resources, Project administration. **David Bartrés-Faz:** Investigation, Resources, Project administration. **Maribel Peró-Cebollero:** Writing – review & editing. **Cristina Cañete-Massé:** Writing – review & editing. **Joan Guàrdia-Olmos:** Conceptualization, Validation, Writing – review & editing, Supervision.

Declaration of competing interest

None.

Data availability

The data is accessible upon request to the authors with the incorporation of the authorization of the local ethical committee for its treatment.

Supplementary materials

Supplementary material associated with this article can be found, in the online version, at doi:10.1016/j.neuroimage.2024.120532.

References

Almgren, H., Van de Steen, F., Kühn, S., Razi, A., Friston, K., Marinazzo, D., 2018. Variability and reliability of effective connectivity within the core default mode network: a multi-site longitudinal spectral DCM study. Neuroimage 183, 757–768. https://doi.org/10.1016/j.neuroimage.2018.08.053.

Andrews-Hanna, J.R., Snyder, A.Z., Vincent, J.L., Lustig, C., Head, D., Raichle, M.E., Buckner, R.L., 2007. Disruption of large-scale brain systems in advanced aging. Neuron 56 (5), 924–935. https://doi.org/10.1016/j.neuron.2007.10.038.

Arc-Chagnaud, C., Millan, F., Salvador-Pascual, A., Correas, A.G., Olaso-Gonzalez, G., De la Rosa, A., Carretero, A., Gomez-Cabrera, M.C., Viña, J., 2019. Reversal of age-associated frailty by controlled physical exercise: the pre-clinical and clinical evidences. Sports Med. Health Sci. 1 (1), 33–39. https://doi.org/10.1016/j.smhs.2019.08.007.

Banks, S.J., Zhuang, X., Bayram, E., Bird, C., Cordes, D., Caldwell, J.Z.K., Cummings, J.L., 2018. Default mode network lateralization and memory in healthy aging and Alzheimer's disease. J. Alzheimer's Dis. 66 (3), 1223–1234. https://doi.org/10.3233/JAD-180541.

Barnes, J., Bartlett, J.W., van de Pol, L.A., Loy, C.T., Scahill, R.I., Frost, C., Thompson, P., Fox, N.C., 2009. A meta-analysis of hippocampal atrophy rates in Alzheimer's disease. Neurobiol. Aging 30 (11), 1711–1723. https://doi.org/10.1016/j.neurobiolaging.2008.01.010.

Beckmann, C.F., DeLuca, M., Devlin, J.T., Smith, S.M., 2005. Investigations into resting-state connectivity using independent component analysis. Philosop. Trans. R. Soc. B Biol. Sci. 360 (1457), 1001–1013. https://doi.org/10.1098/rstb.2005.1634.

Beckmann, C.F., Smith, S.M., 2004. Probabilistic independent component analysis for functional magnetic resonance imaging. IEEE Trans. Med. Imaging 23 (2), 137–152. https://doi.org/10.1109/tmi.2003.822821.

Biswal, B., Zerrin Yetkin, F., Haughton, V.M., Hyde, J.S., 1995. Functional connectivity in the motor cortex of resting human brain using echo-planar mri. Magn. Reson. Med. 34 (4), 537–541. https://doi.org/10.1002/mrm.1910340409.

Buckner, R.L., Andrews-Hanna, J.R., Schacter, D.L., 2008. The brain's default network: anatomy, function, and relevance to disease. Ann. N. Y. Acad. Sci. 1124 (1), 1–38. https://doi.org/10.1196/annals.1440.011.

Buckner, R.L., Snyder, A.Z., Shannon, B.J., LaRossa, G., Sachs, R., Fotenos, A.F., Sheline, Y.I., Klunk, W.E., Mathis, C.A., Morris, J.C., Mintun, M.A., 2005. Molecular, structural, and functional characterization of Alzheimer's disease: evidence for a relationship between default activity, amyloid, and memory. J. Neurosci. 25 (34), 7709–7717. https://doi.org/10.1523/JNEUROSCI.2177-05.2005.

Chen, Y., Qi, D., Qin, T., Chen, K., Ai, M., Li, X., Li, H., Zhang, J., Mao, H., Yang, Y., Zhang, Z., 2018. Brain network connectivity mediates education-related cognitive performance in healthy elderly adults. Curr. Alzheimer Res. 16 (1), 19–28. https://doi.org/10.2174/1567205015666181022094158.

Damoiseaux, J.S., Beckmann, C.F., Arigita, E.J.S., Barkhof, F., Scheltens, P., Stam, C.J., Smith, S.M., Rombouts, S.A.R.B., 2008. Reduced resting-state brain activity in the "default network" in normal aging. Cerebral Cortex 18 (8), 1856–1864. https://doi.org/10.1093/cercor/bhm207.

Damoiseaux, J.S., Prater, K.E., Miller, B.L., Greicius, M.D., 2012. Functional connectivity tracks clinical deterioration in Alzheimer's disease. Neurobiol. Aging 33 (4), 828. https://doi.org/10.1016/j.neurobiolaging.2011.06.024 e19-828.e30.

Damoiseaux, J.S., Viviano, R.P., Yuan, P., Raz, N., 2016. Differential effect of age on posterior and anterior hippocampal functional connectivity. Neuroimage 133, 468–476. https://doi.org/10.1016/j.neuroimage.2016.03.047.

Darlington, R.B., Weinberg, S.L., Walberg, H.J., 1973. Canonical variate analysis and related techniques. Rev. Educ. Res. 43 (4), 433–454. https://doi.org/10.3102/00346543043004433.

Esménio, S., Soares, J.M., Oliveira-Silva, P., Zeidman, P., Razi, A., Gonçalves, Ó.F., Friston, K.J., Coutinho, J., 2019. Using resting-state DMN effective connectivity to characterize the neurofunctional architecture of empathy. Sci. Rep. 9 (1), 2603. https://doi.org/10.1038/s41598-019-38801-6.

Farras-Permanyer, L., Mancho-Fora, N., Montalà-Flaquer, M., Bartrés-Faz, D., Vaqué-Alcázar, L., Peró-Cebollero, M., Guàrdia-Olmos, J., 2019. Age-related changes in resting-state functional connectivity in older adults. Neural Regen. Res. 14 (9), 1544. https://doi.org/10.4103/1673-5374.255976.

Ferreira, L.K., Busatto, G.F., 2013. Resting-state functional connectivity in normal brain aging. Neurosci. Biobehav. Rev. 37 (3), 384–400. https://doi.org/10.1016/j.neubiorev.2013.01.017.

Folstein, M.F., Folstein, S.E., McHugh, P.R., 1975. Mini-mental state": a practical method for grading the cognitive state of patients for the clinician. J. Psychiatr. Res. 12 (3), 189–198. https://doi.org/10.1016/0022-3956(75)90026-6.

Franzmeier, N., Ren, J., Damm, A., Monté-Rubio, G., Boada, M., Ruiz, A., Ramirez, A., Jessen, F., Düzel, E., Rodríguez Gómez, O., Benzinger, T., Goate, A., Karch, C.M., Fagan, A.M., McDade, E., Buerger, K., Levin, J., Duering, M., Dichgans, M., Ewers, M., 2021. The BDNFVal66Met SNP modulates the association between beta-amyloid and hippocampal disconnection in Alzheimer's disease. Mol. Psychiatry 26 (2). https://doi.org/10.1038/s41380-019-0404-6.

Friston, K.J., 2011. Functional and effective connectivity: a review. Brain Connect. 1 (1), 13–36. https://doi.org/10.1089/brain.2011.0008.

Friston, K.J., Harrison, L., Penny, W., 2003. Dynamic causal modelling. Neuroimage 19 (4), 1273–1302. https://doi.org/10.1016/S1053-8119(03)00202-7.

Friston, K.J., Kahan, J., Biswal, B., Razi, A., 2014. A DCM for resting state fMRI. Neuroimage 94, 396–407. https://doi.org/10.1016/j.neuroimage.2013.12.009.

Friston, K.J., Litvak, V., Oswal, A., Razi, A., Stephan, K.E., van Wijk, B.C.M., Ziegler, G., Zeidman, P., 2016. Bayesian model reduction and empirical Bayes for group (DCM) studies. Neuroimage 128, 413–431. https://doi.org/10.1016/j.neuroimage.2015.11.015.

Friston, K.J., Mattout, J., Trujillo-Barreto, N., Ashburner, J., Penny, W., 2007. Variational free energy and the Laplace approximation. Neuroimage 34 (1), 220–234. https://doi.org/10.1016/j.neuroimage.2006.08.035.

Ge, R., Fu, Y., Wang, D., Yao, L., Long, Z., 2014. Age-related alterations of brain network underlying the retrieval of emotional autobiographical memories: an fMRI study using independent component analysis. Front. Hum. Neurosci. 8. https://www.frontiersin.org/articles/10.3389/fnhum.2014.00629.

Harrison, T.M., Maass, A., Adams, J.N., Du, R., Baker, S.L., Jagust, W.J., 2019. Tau deposition is associated with functional isolation of the hippocampus in aging. Nat. Commun. 10 (1), 1. https://doi.org/10.1038/s41467-019-12921-z. Article.

Hartshorne, J.K., Germine, L.T., 2015. When does cognitive functioning peak? The asynchronous rise and fall of different cognitive abilities across the life span. Psychol. Sci. 26 (4), 433–443. https://doi.org/10.1177/0956797614567339.

Hu, S., Chao, H.H.-A., Zhang, S., Ide, J.S., Li, C.-S.R., 2014. Changes in cerebral morphometry and amplitude of low-frequency fluctuations of BOLD signals during healthy aging: Correlation with inhibitory control. Brain Structure and Function 219 (3), 983–994. https://doi.org/10.1007/s00429-013-0548-0.

Jones, D.T., Machulda, M.M., Vemuri, P., McDade, E.M., Zeng, G., Senjem, M.L., Gunter, J.L., Przybelski, S.A., Avula, R.T., Knopman, D.S., Boeve, B.F., Petersen, R.C., Jack, C.R., 2011. Age-related changes in the default mode network are more advanced in Alzheimer disease. Neurology 77 (16), 1524–1531. https://doi.org/10.1212/WNL.0b013e318233b33d.

Kaplan, E., Goodglass, H., Weintrab, S., 1983. The Boston Naming Test. Febiger.

Kaplan, E., Goodglass, H., Weintraub, S., 2001. Boston Naming Test-2, 2nd ed. Austin, TX. Pro-Ed.

Koch, W., Teipel, S., Mueller, S., Buerger, K., Bokde, A.L.W., Hampel, H., Coates, U., Reiser, M., Meindl, T., 2010. Effects of aging on default mode network activity in resting state fMRI: Does the method of analysis matter? Neuroimage 51 (1), 280–287. https://doi.org/10.1016/j.neuroimage.2009.12.008.

Lezak, M.D., Howieson, D.B., Loring, D.W., Fisher, J.S., 2004. Neuropsychological Assessment. Oxford University Press.

Lin, M.-Y., Tseng, Y.-J., Cheng, C.-H., 2018. Age effects on spatiotemporal dynamics of response inhibition: an MEG study. Front. Aging Neurosci. 10. https://www.frontiersin.org/articles/10.3389/fnagi.2018.00386.

Lin, P., Yang, Y., Jovicich, J., De Pisapia, N., Wang, X., Zuo, C.S., Levitt, J.J., 2016. Static and dynamic posterior cingulate cortex nodal topology of default mode network predicts attention task performance. Brain Imaging Behav. 10 (1), 212–225. https://doi.org/10.1007/s11682-015-9384-6.

Liu, R.-M., 2022. Aging, cellular senescence, and Alzheimer's disease. Int. J. Mol. Sci. 23 (4), 1989. https://doi.org/10.3390/ijms23041989.

Lorenzini, L., van Wingen, G., Cerliani, L., 2021. Atypically high influence of subcortical activity on primary sensory regions in autism. NeuroImage Clin. 32, 102839 https://doi.org/10.1016/j.nicl.2021.102839.

Marchitelli, R., Aiello, M., Cachia, A., Quarantelli, M., Cavaliere, C., Postiglione, A., Tedeschi, G., Montella, P., Milan, G., Salvatore, M., Salvatore, E., Baron, J.C., Pappatà, S., 2018. Simultaneous resting-state FDG-PET/fMRI in Alzheimer disease: relationship between glucose metabolism and intrinsic activity. Neuroimage 176, 246–258. https://doi.org/10.1016/j.neuroimage.2018.04.048.

Milton, F., Butler, C.R., Benattayallah, A., Zeman, A.Z.J., 2012. The neural basis of autobiographical memory deficits in transient epileptic amnesia. Neuropsychologia 50 (14), 3528–3541. https://doi.org/10.1016/j.neuropsychologia.2012.09.027.

Montalà-Flaquer, M., Cañete-Massé, C., Vaqué-Alcázar, L., Bartrés-Faz, D., Peró-Cebollero, M., Guàrdia-Olmos, J., 2023. Spontaneous brain activity in healthy aging: An overview through fluctuations and regional homogeneity. Front. Aging Neurosci. 14, 1002811 https://doi.org/10.3389/fnagi.2022.1002811.

Montemurro, S., Filippini, N., Ferrazzi, G., Mantini, D., Arcara, G., Marino, M., 2023. Education differentiates cognitive performance and resting state fMRI connectivity in healthy aging. Front. Aging Neurosci. 15. https://www.frontiersin.org/articles/10.3389/fnagi.2023.1168576.

Mosconi, L., Brys, M., Glodzik-Sobanska, L., De Santi, S., Rusinek, H., de Leon, M.J., 2007. Early detection of Alzheimer's disease using neuroimaging. Exp. Gerontol. 42 (1), 129–138. https://doi.org/10.1016/j.exger.2006.05.016.

Nelson, H.E., 1982. National Adult Reading Test (NART): Test Manual. Nfer-Nelson.

Nelson, H.E., Willison, J., 1991. National Adult Reading Test (NART). Nfer-Nelson.

Nickerson, L.D., Smith, S.M., Öngür, D., Beckmann, C.F., 2017. Using dual regression to investigate network shape and amplitude in functional connectivity analyses. Front. Neurosci. 11 https://doi.org/10.3389/fnins.2017.00115.

Nobis, L., Manohar, S.G., Smith, S.M., Alfaro-Almagro, F., Jenkinson, M., Mackay, C.E., Husain, M., 2019. Hippocampal volume across age: Nomograms derived from over 19,700 people in UK Biobank. NeuroImage: Clinical 23, 101904. https://doi.org/10.1016/j.nicl.2019.101904.

Onoda, K., Ishihara, M., Yamaguchi, S., 2012. Decreased functional connectivity by aging is associated with cognitive decline. J. Cogn. Neurosci. 24 (11), 2186–2198. https://doi.org/10.1162/jocn_a_00269.

Oschwald, J., Guye, S., Liem, F., Rast, P., Willis, S., Röcke, C., Jäncke, L., Martin, M., Mérillat, S., 2019. Brain structure and cognitive ability in healthy aging: a review on longitudinal correlated change. Rev. Neurosci. 31 (1), 1–57. https://doi.org/10.1515/revneuro-2018-0096.

O'Sullivan, M., Jones, D.K., Summers, P.E., Morris, R.G., Williams, S.C.R., Markus, H.S., 2001. Evidence for cortical "disconnection" as a mechanism of age-related cognitive decline. Neurology. 57 (4), 632–638. https://doi.org/10.1212/WNL.57.4.632.

Rabin, J.S., Gilboa, A., Stuss, D.T., Mar, R.A., Rosenbaum, R.S., 2010. Common and unique neural correlates of autobiographical memory and theory of mind. J. Cogn. Neurosci. 22 (6), 1095–1111. https://doi.org/10.1162/jocn.2009.21344.

Raichle, M.E., 2015. The brain's default mode network. Annu Rev. Neurosci. 38 (1), 433–447. https://doi.org/10.1146/annurev-neuro-071013-014030.

Raichle, M.E., MacLeod, A.M., Snyder, A.Z., Powers, W.J., Gusnard, D.A., Shulman, G.L., 2001. A default mode of brain function. Proc. Natl. Acad. Sci. 98 (2), 676–682. https://doi.org/10.1073/pnas.98.2.676.

Raz, N., Rodrigue, K.M., 2006. Differential aging of the brain: Patterns, cognitive correlates and modifiers. Neurosci. Biobehav. Rev. 30 (6), 730–748. https://doi.org/10.1016/j.neubiorev.2006.07.001.

Razi, A., Kahan, J., Rees, G., Friston, K.J., 2015. Construct validation of a DCM for resting state fMRI. Neuroimage 106, 1–14. https://doi.org/10.1016/j.neuroimage.2014.11.027.

Rey, A., 1964. Clinical Tests in Psychology. Presses Universitaires de France.

Sala-Llonch, R., Bartrés-Faz, D., Junqué, C., 2015. Reorganization of brain networks in aging: a review of functional connectivity studies. Front. Psychol. 6 https://doi.org/10.3389/fpsyg.2015.00663.

Salami, A., Pudas, S., Nyberg, L., 2014. Elevated hippocampal resting-state connectivity underlies deficient neurocognitive function in aging. Proc. Natl. Acad. Sci. 111 (49), 17654–17659. https://doi.org/10.1073/pnas.1410233111.

Sambataro, F., Murty, V.P., Callicott, J.H., Tan, H.-Y., Das, S., Weinberger, D.R., Mattay, V.S., 2010. Age-related alterations in default mode network: Impact on working memory performance. Neurobiol. Aging 31 (5), 839–852. https://doi.org/10.1016/j.neurobiolaging.2008.05.022.

Shen, X., Cox, S.R., Adams, M.J., Howard, D.M., Lawrie, S.M., Ritchie, S.J., Bastin, M.E., Deary, I.J., McIntosh, A.M., Whalley, H.C., 2018. Resting-state connectivity and its association with cognitive performance, educational attainment, and household income in the UK biobank. Biol. Psychiatry Cogn. Neurosci. Neuroimaging 3 (10), 878–886. https://doi.org/10.1016/j.bpsc.2018.06.007.

Soares, J.M., Magalhães, R., Moreira, P.S., Sousa, A., Ganz, E., Sampaio, A., Alves, V., Marques, P., Sousa, N., 2016. A Hitchhiker's guide to functional magnetic resonance imaging. Front. Neurosci. 10 https://doi.org/10.3389/fnins.2016.00515.

Stern, Y., 2009. Cognitive reserve. Neuropsychologia 47 (10), 2015–2028. https://doi.org/10.1016/j.neuropsychologia.2009.03.004.

Stern, Y., Arenaza-Urquijo, E.M., Bartrés-Faz, D., Belleville, S., Cantilon, M., Chetelat, G., Ewers, M., Franzmeier, N., Kempermann, G., Kremen, W.S., Okonkwo, O., Scarmeas, N., Soldan, A., Udeh-Momoh, C., Valenzuela, M., Vemuri, P., Vuoksimaa, E., and the Reserve, Resilience and Protective Factors PIA Empirical Definitions and Conceptual Frameworks Workgroup, 2020. Whitepaper: defining and investigating cognitive reserve, brain reserve, and brain maintenance. Alzheimer's Dementia 16 (9), 1305–1311. https://doi.org/10.1016/j.jalz.2018.07.219.

Svoboda, E., McKinnon, M.C., Levine, B., 2006. The functional neuroanatomy of autobiographical memory: a meta-analysis. Neuropsychologia 44 (12), 2189–2208. https://doi.org/10.1016/j.neuropsychologia.2006.05.023.

Tombaugh, T.N., McIntyre, N.J., 1992. The mini-mental state examination: a comprehensive review. J. Am. Geriatr. Soc. 40 (9), 922–935. https://doi.org/10.1111/j.1532-5415.1992.tb01992.x.

Torres, D.M.C., Cardenas, F.P., 2020. Synaptic plasticity in Alzheimer's disease and healthy aging. Rev. Neurosci. 31 (3), 245–268. https://doi.org/10.1515/revneuro-2019-0058.

Vaqué-Alcázar, L., Sala-Llonch, R., Abellaneda-Pérez, K., Coll-Padrós, N., Valls-Pedret, C., Bargalló, N., Ros, E., Bartrés-Faz, D., 2020. Functional and structural correlates of working memory performance and stability in healthy older adults. Brain Struct. Funct. 225 (1), 375–386. https://doi.org/10.1007/s00429-019-02009-1.

Vogelaere, F., Santens, P., Achten, E., Boon, P., Vingerhoets, G., 2012. Altered default-mode network activation in mild cognitive impairment compared with healthy aging. Neuroradiology. 54 (11), 1195–1206. https://doi.org/10.1007/s00234-012-1036-6.

Wang, S., Tepfer, L., Taren, A.A., Smith, D.V., 2020. Functional parcellation of the default mode network: a large-scale meta-analysis. Sci. Rep. 10 (1) https://doi.org/10.1038/s41598-020-72317-8.

Watanabe, H., Bagarinao, E., Maesawa, S., Hara, K., Kawabata, K., Ogura, A., Ohdake, R., Shima, S., Mizutani, Y., Ueda, A., Ito, M., Katsuno, M., Sobue, G., 2021. Characteristics of neural network changes in normal aging and early dementia. Front. Aging Neurosci. 13, 747359 https://doi.org/10.3389/fnagi.2021.747359.

World Health Organization, 2022. Ageing and Health. October 1. WHO. https://www.who.int/news-room/fact-sheets/detail/ageing-and-health.

Wimber, M., Heinze, H.-J., Richardson-Klavehn, A., 2010. Distinct frontoparietal networks set the stage for later perceptual identification priming and episodic recognition memory. J. Neurosci. 30 (40), 13272–13280. https://doi.org/10.1523/JNEUROSCI.0588-10.2010.

Yarkoni, T., Poldrack, R.A., Nichols, T.E., Van Essen, D.C., Wager, T.D., 2011. Large-scale automated synthesis of human functional neuroimaging data. Nat. Methods 8 (8), 665–670. https://doi.org/10.1038/nmeth.1635.

Yu, H., Qu, H., Chen, A., Du, Y., Liu, Z., Wang, W., 2021. Alteration of effective connectivity in the default mode network of autism after an intervention. Front. Neurosci. 15, 796437 https://doi.org/10.3389/fnins.2021.796437.

Zeidman, P., Jafarian, A., Corbin, N., Seghier, M.L., Razi, A., Price, C.J., Friston, K.J., 2019a. A guide to group effective connectivity analysis, part 1: First level analysis with DCM for fMRI. Neuroimage 200, 174–190. https://doi.org/10.1016/j.neuroimage.2019.06.031.

Zeidman, P., Jafarian, A., Seghier, M.L., Litvak, V., Cagnan, H., Price, C.J., Friston, K.J., 2019b. A guide to group effective connectivity analysis, part 2: Second level analysis

with PEB. Neuroimage 200, 12–25. https://doi.org/10.1016/j.neuroimage.2019.06.032.